AIMS Mathematics, 11(11): 36163–36187.
DOI: 10.3934/math.20261401
Received: 18 August 2026
Revised: 10 October 2026
Accepted: 15 October 2026
Published: 04 November 2026

https://www.aimspress.com/journal/Math

Research article

Steering semilinear beam dynamics with memory, delay, and non-instantaneous impulses: Approximate controllability and numerical evidence

Boshra K. Alarfaj[1,*], Kawther K. Alarfaj[2], Fatema Al Najim[2] and Maryam Khalid Alarfaj[3]

[1] Department of Statistics and Operations Research, College of Science, King Saud University, P.O. Box 2455, Riyadh 11451, Saudi Arabia

[2] Department of Mathematics and Statistics, College of Science, King Faisal University, P.O. Box 400, Al-Ahsa 31982, Saudi Arabia

[3] School of Computer Science, Faculty of Engineering and Information Technology, University of Technology Sydney, NSW, Australia

* **Correspondence:** Email: Balarfaj@ksu.edu.sa.

Abstract: A conditional approximate-controllability framework is developed for a semilinear Euler–Bernoulli beam with delay, hereditary memory, and non-instantaneous impulses in a product Hilbert space. The linear steering mechanism uses a short terminal control window and a Tikhonov-regularized controllability Gramian. With this window shorter than the delay and located after the final impulse, the delayed nonlinear contributions are determined by the preceding history. We identify hypotheses under which these residuals vanish and exclude an earlier inappropriate vanishing-control-energy requirement. To provide corresponding numerical evidence, MATLAB R2025b calculations use a spatially distributed Gramian controller for every finite-difference beam mode, coupled with an implicit-midpoint structural scheme, nonlinear delayed forcing, exponentially fading memory, and a finite-duration impulse. The computed displacement, velocity, and full product-energy terminal errors decrease under regularization (from 2.2050 to 3.3683×10^{-5} in the full product norm), while control cost rises. Direct full-grid propagation agrees with the Gramian residual prediction at the reported precision. These calculations support the specified finite-grid, control-affine benchmark; they do not themselves prove the infinite-dimensional theorem.

Keywords: semilinear beam equation; non-instantaneous impulses; approximate controllability; time delay; semigroup theory; memory effects
Mathematics Subject Classification: 74K10, 93B05, 35L75

1. Introduction

Equations for beams play a significant role in the development of mathematical models for elastic bodies including suspension bridges, airplane wings, and skyscrapers under dynamical loads. The classical Euler–Bernoulli formulation treats present displacement and velocity, whereas the additional hereditary and delayed mechanisms considered below introduce dependence on past states. For background on nonlinear beam dynamics and related mechanical formulations, see [1–3]. This approach does not account for two classes of behavior of the physical system: firstly, impulses distributed in time; and secondly, delayed behavior due to memory of the system. The aim of this paper is to study the problem of approximate controllability of the equation describing a beam with the above features.

The non-instantaneous impulse effect appears in various practical applications. For instance, the redistribution of the tension in the cables of a suspension bridge due to the load jump is not instantaneous but occurs within a relaxation period that is a function of the stiffness of the cables and the anchorage compliance. In another case, in the active vibration control of flexible structures, where there is saturation of the control actuator or rate limitations, the control force appears gradually rather than instantly. In order to mathematically model the above cases, one needs the notion of non-instantaneous impulses, which was introduced formally in [4]. Non-instantaneous impulses differ from the impulsive differential equations discussed in [5] since the impulsive function acts in the interval $(\ell_k, \vartheta_k]$. Further existence and optimal-control questions under non-instantaneous impulses have been examined in [6].

Delay and memory aspects have a long tradition in structural mechanics. The viscoelasticity of beam materials, for example, gives rise to stress relaxation in such a way that, under constant strain, the stress decreases according to a hereditary integral. This property is explicitly modeled by the Boltzmann superposition principle through the inclusion of a convolution with respect to the kernel g, and leads immediately to the form of the integro-differential operator seen in our model. Delay arises when the system is subject to external forcing through a feedback loop with a certain delay involved in the process, as in remote structural health monitoring.

The controllability problem for beam equations has been investigated using various approaches. Classical controllability theory for distributed-parameter and elastic systems provides essential background: Zuazua treated the semilinear wave equation [7], whereas Lagnese and Lions developed plate models and their analysis and control [8]. These works concern related, but not identical, evolution equations. In the case of semilinear beams, the approximate controllability was proven by Carrasco, Leiva, and Sanchez [9], where an abstract semigroup setting was used, and the authors found sufficient conditions for the nonlinearity such that the approximation through linearization provides the required density. Controllability problems for systems of equations with instantaneous impulses in Hilbert spaces have been considered in [10], whereas related forced-oscillation results for impulsive Euler–Bernoulli beam equations with damping have been reported by Priyadharshini et al. [11]. In the case of impulsive and delay systems, the approximate controllability problem has been solved in [12] through the resolvent approach. The numerical treatment of the controllability for parabolic equations with impulses has been studied in [13]. Other pertinent developments include mild-solution analysis for fractional non-instantaneous impulses [14], Hilfer fractional controllability with non-instantaneous impulses [15], and approximate controllability for Sobolev-type fractional

delay systems [16]. Related, but operator-specific, exact or conformable controllability results appear in [17, 18].

A particularly relevant recent development is the 2026 study of Guo, Zhang, and Li [19], which establishes controllability criteria for a tempered fractional-order evolution problem with nonlocal delay and impulsive conditions. Their attenuation kernel and fractional solution operators differ from the integer-order damped beam semigroup used here; the paper is therefore a closely related contribution to the memory–impulse–delay literature, not a proof for the present beam. Earlier, Kumar [20] considered fractional nonlocal impulsive semilinear systems with time-varying delay; Arora, Mohan, and Dabas [21] studied approximate controllability for fractional functional evolution equations with state-dependent delay and non-instantaneous impulses; and Kumar et al. [22] treated neutral fractional integro-differential inclusions with infinite delay and non-instantaneous impulses. These works employ fractional resolvent or fixed-point techniques and establish useful precedents for the coexistence of nonlocal memory, delay, and impulse effects. The distinguishing feature of the present paper is the terminal-window freezing argument for a damped Euler–Bernoulli beam, together with a finite-grid Gramian steering experiment; no direct equivalence between these different fractional and classical generators is asserted.

To the best of our knowledge, the specific combination of this damped-beam setting, reset-memory convention, terminal delay freezing, and interval-impulse steering is not covered by the cited articles; this is a qualified statement about the precise model and proof mechanism, not a claim that memory–delay–impulse controllability is absent from the literature. These effects require a piecewise, history-dependent solution description: Interval impulses prescribe an alternate evolution rule on their active intervals, and hereditary and delayed terms introduce dependence on past states. They do not destroy the C_0-semigroup property of the underlying linear beam generator, which remains the principal propagation operator between impulses. Taking into account all these phenomena, we need to use another form of the problem statement in the product Hilbert space $\mathbb{U} = \mathbb{X}^1 \times \mathbb{X}$.

Motivated by these considerations, we study the following semilinear beam system on a bounded domain $\Omega \subseteq \mathbb{R}^N$:

$$\aleph'' - 2\gamma\Delta\aleph' + \Delta^2\aleph = u + f(\ell, \aleph(\ell - a), \aleph'(\ell - a), u) + \int_{\vartheta_i}^{\ell} g(\ell - \vartheta)h(\aleph(\vartheta - a, \varpi))\,\mathrm{d}\vartheta, \quad \text{in } \bigcup_{i=0}^{N}(\vartheta_i, \ell_{i+1}],$$

subject to boundary and initial conditions and non-instantaneous impulses:

$$\begin{cases} \aleph(\ell, \varpi) = \Delta\aleph(\ell, \varpi) = 0, & \text{on } \partial\Omega, \\ \aleph(\vartheta, \varpi) = \varphi_1(\vartheta, \varpi), & \text{in } [-a, 0], \\ \aleph'(\vartheta, \varpi) = \varphi_2(\vartheta, \varpi), & \text{in } [-a, 0], \\ \aleph'(\ell, \varpi) = v_i(\ell, \varpi), \quad \aleph(\ell, \varpi) = \aleph(\ell_i^-, \varpi) + \int_{\ell_i}^{\ell} v_i(s, \varpi)\,ds, & \text{in } \bigcup_{i=1}^{N}(\ell_i, \vartheta_i]. \end{cases}$$

Here $\aleph(\ell, \varpi)$ denotes the transverse beam deflection, $\gamma > 1$ is the damping coefficient, $u \in L^2(0, L; \mathbb{X})$ with $\mathbb{X} = L^2(\Omega)$ is the distributed control, and $0 = \vartheta_0 = \ell_0 < \ell_1 \le \vartheta_1 < \cdots < \ell_N \le \vartheta_N < \ell_{N+1} = L$. The function g is the convolution memory kernel, f encodes the nonlinear perturbations, and ψ_i describes the non-instantaneous impulsive response

active on $(\ell_k, \vartheta_k]$. The pair (φ_1, φ_2) prescribes the initial history on $[-a, 0]$. Throughout, the control takes values in $\mathbb{X} = L^2(\Omega)$ and acts on the system only through the operator $\mathbb{B} : \mathbb{X} \to \mathbb{U}$ introduced in Section 2, which embeds it into the velocity component of the product state. The state itself evolves in $\mathbb{U} = \mathbb{X}^1 \times \mathbb{X}$.

The three nonclassical mechanisms appearing in the model play different mathematical roles and it is useful to distinguish them from the beginning. The delay a means that the value entering the nonlinear term at the current time ℓ is the previously generated state $\aleph(\ell - a)$ and its velocity. The hereditary term is different: It accumulates the whole previous evolution through a Volterra convolution, so even after the delay value is fixed, the memory term still carries an integral contribution. Finally, a non-instantaneous impulse does not act at one isolated time. Instead, during the whole interval $(\ell_i, \vartheta_i]$, the evolution is prescribed by the impulse law ψ_i. Consequently, the state space must simultaneously keep track of the beam energy, the recent delayed history, and the piecewise dynamics created by the impulse intervals.

Approximate rather than exact controllability is the natural notion in the present infinite-dimensional setting. Since the beam semigroup is compact for positive times, the corresponding controllability operator is compact as well and therefore cannot be onto an infinite-dimensional Hilbert space. Nevertheless, its range may be dense. This density is sufficient for approximate controllability: Every target can be reached with an arbitrarily small terminal error. The controllability Gramian and its Tikhonov regularization provide a convenient way to quantify this dense-range property and to construct a family of approximate steering controls.

The basic notion used in the paper from the analysis perspective is the use of a small terminal control time window. For some $\beta > 0$ such that $\beta < a$, we use the final steering control on the time interval $[L - \beta, L]$ only. Indeed, if $\ell \in [L - \beta, L]$, then $\ell - a < L - \beta$; therefore, the history entering the nonlinearity has already been formed prior to the terminal control action. This simple observation is crucial: It allows separating the terminal linear steering process from the history dependence and estimating the nonlinear term on a very small interval. See Lemma 4.2 in Section 4.

The contributions of this work can therefore be summarized more precisely as follows. First, the Euler–Bernoulli beam with damping, finite delay, hereditary memory, and non-instantaneous impulses is written as a first-order evolution equation on the product Hilbert space $\mathbb{U} = \mathbb{X}^1 \times \mathbb{X}$. Second, the controllability map and Gramian of the associated linear problem are recalled, and their regularized steering formula is explained in detail. Third, the short-window history-freezing argument is isolated as a separate lemma, which clarifies why the delay does not destroy the final steering mechanism. Fourth, sufficient hypotheses are stated explicitly for the nonlinear and memory remainders, with unrestricted direct dependence on the control excluded unless it is absorbed into a suitable affine control operator. Finally, a full-spatial-grid implementation of Tikhonov-regularized Gramian steering is provided for a specified control-affine, delayed, and impulsive beam benchmark. It computes all terminal-state components, compares the predicted and propagated residuals, and tests mesh refinement and parameter sensitivity. These finite-grid results supplement, but cannot replace, the Hilbert-space proof.

Unlike the instantaneous impulses in [10] or the beam-specific setting in [9], the terminal-window device here isolates a known delayed trajectory while retaining a reset-memory residual and an explicit interval impulse law. This is a structural sufficient-condition argument, not a blanket result for all control-dependent nonlinearities. In structural engineering, g may represent viscoelastic

relaxation; the finite delay may model sensor–actuator latency in flexible arms, bridges, or aerospace structures; and an interval impulse may represent a finite-time actuator intervention rather than a mathematical jump. These examples are motivations, not parameter calibrations to an engineering device. Extensions to Timoshenko beams and plates require generation/dense-range results for their own first-order operators and appropriate regularity of impulse maps; weakly damped wave or fractional models need new propagator and terminal estimates.

The remainder of the paper is organized as follows. Section 2 develops the functional-analytic and piecewise mild-solution framework. Section 3 reviews the linear Gramian and regularized steering mechanism. Section 4 proves the semilinear approximate-controllability result and explains the terminal-window compatibility condition. Section 5 gives the numerical methodology and computational evidence, while Section 6 discusses the scope of the assumptions. The final section summarizes the conclusions.

2. Functional analytic formulation of the beam problem

This is to ensure that we clearly outline how the beam equation of second order is reduced to a first order evolution equation as well as how the delay, memory, and impulse terms feature in the abstract form. The reason for doing this is that the controllability results of Sections 3 and 4 are stated within the product Hilbert space.

2.1. The positive beam operator and fractional power spaces

Assume that $\Omega \subset \mathbb{R}^N$ is bounded with C^2 boundary; use a smooth boundary to interpret fourth-order traces. Let

$$\mathbb{X} = L^2(\Omega)$$

and let $\mathbb{A}_0 = -\Delta$ be the positive Dirichlet Laplacian with domain

$$D(\mathbb{A}_0) = H^2(\Omega) \cap H_0^1(\Omega).$$

The subscript in $\mathbb{A}_0$ is used deliberately: $\mathbb{A}_0$ is the spatial elliptic operator, while the block operator governing the first-order beam dynamics will be denoted by $\mathbb{A}$. This distinction avoids the ambiguity that arises if the same symbol is used for both operators.

Since Ω is bounded, $\mathbb{A}_0$ has compact resolvent. Hence there exist positive eigenvalues

$$0 < \mu_1 < \mu_2 < \cdots, \qquad \mu_j \longrightarrow \infty,$$

with finite multiplicities γ_j, orthonormal eigenfunctions $\{\phi_{j_k}\}$, and spectral projections E_j such that

$$\mathbb{A}_0\varpi = \sum_{j=1}^{\infty} \mu_j E_j \varpi, \qquad \varpi \in D(\mathbb{A}_0). \tag{2.1}$$

The analytic semigroup generated by $-\mathbb{A}_0$ is therefore

$$S_0(\ell)\varpi = \sum_{j=1}^{\infty} e^{-\mu_j \ell} E_j \varpi, \qquad \|S_0(\ell)\| \le e^{-\mu_1 \ell}. \tag{2.2}$$

For $\rho \geq 0$, define the fractional power space

$$\mathbb{X}^{\rho} = D(\mathbb{A}_0^{\rho}) = \left\{ \varpi \in \mathbb{X} : \sum_{j=1}^{\infty} \mu_j^{2\rho} \|E_j \varpi\|^2 < \infty \right\}, \tag{2.3}$$

endowed with the graph norm

$$\|\varpi\|_{\mathbb{X}^{\rho}} = \|\mathbb{A}_0^{\rho} \varpi\|_{\mathbb{X}}.$$

For $\rho > 0$, $\mathbb{X}^{\rho}$ is continuously and densely embedded in $\mathbb{X}$. In particular,

$$\mathbb{X}^{1/2} \hookrightarrow \mathbb{X}, \qquad \overline{\mathbb{X}^{1/2}}^{\mathbb{X}} = \mathbb{X}.$$

The equality above is a density statement; it does not identify the two normed spaces.

The natural beam energy space is

$$\mathbb{U} = \mathbb{X}^1 \times \mathbb{X}, \qquad \|(x, y)\|_{\mathbb{U}}^2 = \|x\|_{\mathbb{X}^1}^2 + \|y\|_{\mathbb{X}}^2. \tag{2.4}$$

The first component represents displacement and the second component velocity.

2.2. First-order product-space formulation

Introduce the state

$$\omega(\ell) = \begin{pmatrix} \aleph(\ell) \\ \aleph'(\ell) \end{pmatrix} \in \mathbb{U} \tag{2.5}$$

and define the block operator

$$\mathbb{A} = \begin{pmatrix} 0 & -I_{\mathbb{X}} \\ \mathbb{A}_0^2 & 2\gamma \mathbb{A}_0 \end{pmatrix}, \qquad D(\mathbb{A}) = \mathbb{X}^2 \times \mathbb{X}^1. \tag{2.6}$$

For smooth $\partial\Omega$, the spectral domain $D(\mathbb{A}_0^2) = \{v \in D(\mathbb{A}_0) : \mathbb{A}_0 v \in D(\mathbb{A}_0)\}$ realizes the hinged (Navier) boundary conditions $v = \Delta v = 0$ in the trace sense. This identification depends on elliptic regularity and must not be inferred from boundedness of Ω alone. The first-order equation

$$\omega'(\ell) + \mathbb{A}\omega(\ell) = \begin{pmatrix} 0 \\ \text{forcing} \end{pmatrix}$$

is exactly the product-space form of the damped second-order beam equation.

The operator $-\mathbb{A}$ generates a strongly continuous compact semigroup $\{S(\ell)\}_{\ell \geq 0}$ on $\mathbb{U}$; see [9]. We shall use the estimate

$$\|S(\ell)\|_{\mathbb{L}(\mathbb{U})} \leq N e^{-\mu \ell}, \qquad \ell \geq 0, \tag{2.7}$$

for constants $N \geq 1$ and $\mu > 0$. The symbol μ in (2.7) denotes the decay rate of the product-space semigroup; it must not be confused with the spectral values μ_j in (2.1). The parameter r_1, introduced later, is reserved exclusively for Tikhonov regularization.

2.3. Delay histories, memory, and non-instantaneous impulses

For a trajectory $\omega : [-a, L] \to \mathbb{U}$, define the history segment at time ℓ by

$$\omega_\ell(\theta) = \omega(\ell + \theta), \qquad -a \le \theta \le 0. \tag{2.8}$$

Thus the delayed value used in the beam equation is simply

$$\omega_\ell(-a) = \omega(\ell - a).$$

This notation is important in the controllability proof because, on a terminal interval shorter than the delay, $\omega(\ell - a)$ belongs to the already computed portion of the trajectory.

Let

$$0 = \vartheta_0 = \ell_0 < \ell_1 \le \vartheta_1 < \cdots < \ell_N \le \vartheta_N < \ell_{N+1} = L.$$

The open intervals $(\vartheta_i, \ell_{i+1}]$ are evolution intervals, whereas $(\ell_i, \vartheta_i]$ are impulse intervals. During an impulse interval, the velocity is not obtained by solving the differential equation; it is prescribed by the impulse law ψ_i. This is the defining difference between an instantaneous impulse and a non-instantaneous one.

The operators entering the abstract system are

$$\mathbb{B}u = \begin{pmatrix} 0 \\ u \end{pmatrix}, \tag{2.9}$$

$$\mathbb{F}(\ell, \eta, u) = \begin{pmatrix} 0 \\ f(\ell, \eta^1(-a), \eta^2(-a), u) \end{pmatrix}, \tag{2.10}$$

$$\mathbb{H}(\ell, \vartheta, \eta) = \begin{pmatrix} 0 \\ g(\ell - \vartheta) h(\eta^1(-a)) \end{pmatrix}. \tag{2.11}$$

On an impulse interval, the velocity is *prescribed explicitly*, rather than determined through an implicit fixed-point equation involving itself. Write $x_i = \omega^1(\ell_i^-)$ and prescribe $v_i \in C([\ell_i, \vartheta_i]; \mathbb{X}^1)$, depending only on the already attained state, past history, and an admissible impulse input via a causal rule. Set

$$\mathcal{J}_i(\ell; x_i, v_i) = \begin{pmatrix} x_i + \displaystyle\int_{\ell_i}^{\ell} v_i(s)\, ds \\ v_i(\ell) \end{pmatrix}, \qquad \ell \in (\ell_i, \vartheta_i]. \tag{2.12}$$

The prescribed v_i is strongly measurable and bounded in $\mathbb{X}^1$; if it depends on an L^2 impulse input, the dependence must be through a bounded causal operator of its restriction to $[\ell_i, \ell]$, never through a point value $u(\vartheta_i)$. The explicit construction avoids the tautology $x = x$ and an unsolvable velocity equation $v = v + e$. It also ensures that the displacement remains in $\mathbb{X}^1$. Compatibility or specified one-sided jumps at the endpoints is part of the impulse data. The distributed control operator $\mathbb{B} \in \mathbb{L}(\mathbb{X}, \mathbb{U})$ injects input into the velocity equation on evolution intervals.

With this notation, the complete abstract system is

$$\begin{cases} \omega'(\ell) + \mathbb{A}\omega(\ell) = \mathbb{B}u(\ell) + \mathbb{F}(\ell, \omega_\ell, u(\ell)) + \displaystyle\int_{\sigma_i}^{\ell} \mathbb{H}(\ell, \vartheta, \omega_\vartheta)\, d\vartheta, & \ell \in (\vartheta_i, \ell_{i+1}], \\ \omega(\ell) = \Phi(\ell), & -a \le \ell \le 0, \\ \omega(\ell) = \mathcal{J}_i(\ell; x_i, v_i), & \ell \in (\ell_i, \vartheta_i], \end{cases} \tag{2.13}$$

where $\sigma_0 = 0$ and, under the reset-memory convention used here, $\sigma_i = \vartheta_i$ for $i \geq 1$.

The hereditary contribution has Volterra form. The present model adopts a reset-memory convention: On each evolution interval $(\vartheta_i, \ell_{i+1}]$ following an impulse, the convolution starts at ϑ_i, and on the first evolution interval it starts at 0. Retaining memory through impulses would require a different piecewise mild formulation, hereditary bounds, and numerical recursion. The persistent-memory alternative is not analyzed in this manuscript.

To make the well-posedness and terminal estimates transparent, we record the basic regularity assumptions used in the remainder of the paper.

Assumption 2.1. *The following conditions are imposed.*

(1) $\mathbb{B} \in \mathbb{L}(\mathbb{X}, \mathbb{U})$*, and* $-\mathbb{A}$ *satisfies* (2.7).

(2) The evolution forcing is Carathéodory, globally Lipschitz in its two delayed state arguments, and has at most linear growth in those arguments and the L^2 *control. The Lipschitz estimates use the piecewise-continuous history space with one-sided switch evaluations.*

(3) $g \in L^1(0, L)$ *and* $h : \mathbb{X}^1 \to \mathbb{X}$ *is globally Lipschitz with at most linear growth. The reset-memory convolution is consequently well defined for bounded histories.*

(4) For each impulse, the prescribed profile v_i *and its causal construction in* (2.12) *are given explicitly and bounded/Lipschitz in the pre-impulse data, with* $v_i \in C([\ell_i, \vartheta_i]; \mathbb{X}^1)$*. The impulse law does not require choosing representatives of* L^2 *controls at isolated time points.*

(5) The initial history $\Phi = (\varphi_1, \varphi_2)$ *belongs to* $C([-a, 0]; \mathbb{U})$*. The full post-impulse history is interpreted in* $\mathbb{PC}$*, with prescribed one-sided traces.*

For a fixed admissible evolution control, global Lipschitz estimates give unique mild evolution on every evolution interval by the standard Volterra argument; the explicit impulse formula then uniquely determines the next impulse interval. Induction over the finitely many intervals and linear growth prevent finite-time explosion. No implicit solvability claim is made for an arbitrary $\Psi_i(\ell, \omega_\ell, u(\ell))$. Related abstract frameworks are discussed in [4, 5, 23]. The controllability theorem will add a more specific terminal-window bound in Section 4.

Definition 2.2 (Piecewise mild solution)**.** *Let* $\mathbb{PC}([-a, L]; \mathbb{U})$ *denote the space of functions that are continuous on every evolution and impulse subinterval and possess the appropriate one-sided limits at switching points. A function* $\omega \in \mathbb{PC}([-a, L]; \mathbb{U})$ *is a mild solution if*

$$\omega(\ell) = \Phi(\ell), \qquad -a \leq \ell \leq 0,$$

and, on the first evolution interval,

$$\begin{aligned} \omega(\ell) = S(\ell)\Phi(0) &+ \int_0^\ell S(\ell - \vartheta)\mathbb{B}u(\vartheta)\, d\vartheta \\ &+ \int_0^\ell S(\ell - \vartheta)\mathbb{F}(\vartheta, \omega_\vartheta, u(\vartheta))\, d\vartheta \\ &+ \int_0^\ell S(\ell - \vartheta) \int_0^\vartheta \mathbb{H}(\vartheta, m, \omega_m)\, dm\, d\vartheta, \qquad 0 \leq \ell \leq \ell_1. \end{aligned} \tag{2.14}$$

On an impulse interval,

$$\omega(\ell) = \mathcal{J}_i(\ell; x_i, v_i), \qquad \ell_i < \ell \le \vartheta_i, \tag{2.15}$$

and on the following evolution interval,

$$\begin{aligned}\omega(\ell) = S(\ell-\vartheta_i)\mathcal{J}_i(\vartheta_i; x_i, v_i) &+ \int_{\vartheta_i}^{\ell} S(\ell-\vartheta)\mathbb{B}u(\vartheta)\,d\vartheta \\ &+ \int_{\vartheta_i}^{\ell} S(\ell-\vartheta)\mathbb{F}(\vartheta, \omega_\vartheta, u(\vartheta))\,d\vartheta \\ &+ \int_{\vartheta_i}^{\ell} S(\ell-\vartheta)\int_{\vartheta_i}^{\vartheta} \mathbb{H}(\vartheta, m, \omega_m)\,dm\,d\vartheta, \qquad \vartheta_i < \ell \le \ell_{i+1}.\end{aligned} \tag{2.16}$$

Remark 2.3. *Formulas* (2.14)–(2.16) *distinguish four different terms. The semigroup moves the state created at the start of the time interval of evolution; the first convolution term represents the distributed control; the second convolution is a semilinear delay perturbation; and the double convolution term is the hereditary memory term. The explicit impulse relation* (2.15) *becomes the law of evolution for time* $(\ell_i, \vartheta_i]$*. It follows that the piecewise formulation is not just a technical issue; it corresponds to the real switching structure of the model.*

Proposition 2.4 (A local terminal bound)**.** *Assume Assumption 2.1. Let* $I = [c, d] \subset (\vartheta_N, L]$ *be an evolution interval and suppose the trajectory remains in a bounded subset of* $\mathbb{U}$ *on* $[c - a, d]$*. Then there exist finite constants* $M_F(I)$ *and* $M_H(I)$*, depending on that bounded set and on the data, such that*

$$\left\| \int_c^d S(d-\vartheta)\mathbb{F}(\vartheta, \omega_\vartheta, u(\vartheta))\,d\vartheta \right\| \le N \int_c^d \|\mathbb{F}(\vartheta, \omega_\vartheta, u(\vartheta))\|\,d\vartheta, \tag{2.17}$$

$$\left\| \int_c^d S(d-\vartheta)\int_{\vartheta_N}^{\vartheta} \mathbb{H}(\vartheta, m, \omega_m)\,dm\,d\vartheta \right\| \le N M_H(I)(d-c). \tag{2.18}$$

If $\mathbb{F}$ *is uniformly bounded on the relevant terminal history set, the first term is also* $O(d-c)$*.*

Proof. The semigroup estimate (2.7) gives $\|S(d-\vartheta)\| \le N$ for $\vartheta \in [c, d]$, which proves (2.17). For the memory term, continuity of h, boundedness of the trajectory, and $g \in L^1$ imply a finite bound for the inner Volterra integral. Integrating this bound over an interval of length $d - c$ proves (2.18). □

3. Controllability of the linear beam equation

The semilinear proof is based on a linear steering problem posed only on the last portion of the time interval. We therefore review the corresponding control operator and, in particular, explain why the regularized Gramian formula produces approximate terminal steering.

Given $\omega_0 \in \mathbb{U}$, $\ell_0 \in [0, L]$, and $u \in L^2(\ell_0, L; \mathbb{X})$, consider

$$\omega'(\ell) = -\mathbb{A}\omega(\ell) + \mathbb{B}u(\ell), \qquad \omega(\ell_0) = \omega_0. \tag{3.1}$$

Its mild solution is

$$\omega(\ell) = S(\ell-\ell_0)\omega_0 + \int_{\ell_0}^{\ell} S(\ell-\vartheta)\mathbb{B}u(\vartheta)\,d\vartheta. \tag{3.2}$$

Definition 3.1 (Approximate controllability of the linear system)**.** *System* (3.1) *is approximately controllable on* $[\ell_0, L]$ *if, for every initial state* $\omega_0 \in \mathbb{U}$*, every target* $\widetilde{\omega} \in \mathbb{U}$*, and every* $\varepsilon > 0$*, there exists* $u \in L^2(\ell_0, L; \mathbb{X})$ *such that*

$$\|\omega(L) - \widetilde{\omega}\|_{\mathbb{U}} < \varepsilon.$$

Unlike exact controllability, Definition 3.1 only requires the reachable set to be dense. This is particularly appropriate here because compactness of $S(\ell)$ for $\ell > 0$ implies compactness of the finite-time control map under the present bounded-control setting, and a compact operator cannot be surjective onto an infinite-dimensional Hilbert space unless its range is finite dimensional.

Definition 3.2 (Terminal control map and Gramian)**.** *For* $\delta \in (0, L]$*, define*

$$G_{L\delta} : L^2(L-\delta, L; \mathbb{X}) \longrightarrow \mathbb{U}, \qquad G_{L\delta}u = \int_{L-\delta}^{L} S(L-\vartheta)\mathbb{B}u(\vartheta)\, d\vartheta. \tag{3.3}$$

Its adjoint is

$$(G_{L\delta}^* z)(\vartheta) = \mathbb{B}^* S^*(L-\vartheta)z, \qquad L-\delta \le \vartheta \le L, \tag{3.4}$$

and the controllability Gramian is

$$Q_{L\delta} = G_{L\delta}G_{L\delta}^*, \qquad Q_{L\delta}z = \int_{L-\delta}^{L} S(L-\vartheta)\mathbb{B}\mathbb{B}^* S^*(L-\vartheta)z\, d\vartheta. \tag{3.5}$$

Proposition 3.3 (Basic Gramian properties)**.** *For every* $\delta > 0$*,* $Q_{L\delta}$ *is bounded, self-adjoint and nonnegative. Moreover,*

$$\langle Q_{L\delta}z, z\rangle_{\mathbb{U}} = \int_{L-\delta}^{L} \|\mathbb{B}^* S^*(L-\vartheta)z\|_{\mathbb{X}}^2\, d\vartheta. \tag{3.6}$$

Consequently, $Q_{L\delta}z = 0$ *if and only if* $\mathbb{B}^* S^*(L-\vartheta)z = 0$ *for almost every* $\vartheta \in [L-\delta, L]$*.*

Proof. Boundedness follows from (2.7), boundedness of $\mathbb{B}$, and the finite length of the interval. Since $Q_{L\delta} = G_{L\delta}G_{L\delta}^*$, it is self-adjoint and nonnegative. Identity (3.6) is obtained from

$$\langle G_{L\delta}G_{L\delta}^* z, z\rangle = \langle G_{L\delta}^* z, G_{L\delta}^* z\rangle_{L^2}.$$

The final statement is immediate because the integrand in (3.6) is nonnegative. □

Lemma 3.4 (Dense-range characterization; see [24–26])**.** *The following assertions are equivalent:*

(i) system (3.1) *is approximately controllable on* $[L-\delta, L]$*;*

(ii) $\overline{\mathrm{Range}(G_{L\delta})} = \mathbb{U}$*;*

(iii) $\mathbb{B}^* S^*(L-\vartheta)z = 0$ *for almost every* $\vartheta \in [L-\delta, L]$ *implies* $z = 0$*;*

(iv) $\langle Q_{L\delta}z, z\rangle > 0$ *for every nonzero* $z \in \mathbb{U}$*;*

(v)

$$\lim_{r_1 \downarrow 0} r_1(r_1 I + Q_{L\delta})^{-1} z = 0 \quad \text{for every } z \in \mathbb{U}. \tag{3.7}$$

Remark 3.5. *The parameter $r_1 > 0$ in* (3.7) *is a Tikhonov regularization parameter. It prevents inversion of a possibly non-invertible compact Gramian. Approximate controllability is expressed by the fact that the regularization defect $r_1(r_1 I + Q_{L\delta})^{-1}$ converges strongly to zero.*

The beam control pair considered in [9] satisfies the dense-range condition. We use that fact in the following form. For the distributed beam input, the short-window assertion can also be seen modewise. For each Dirichlet eigenmode μ_j, the damped displacement–velocity pair has matrix $A_j = \left(\begin{smallmatrix} 0 & 1 \\ -\mu_j^2 & -2\gamma\mu_j \end{smallmatrix}\right)$ and column $B_j = (0,1)^T$. The Kalman matrix $[B_j, A_j B_j] = \left(\begin{smallmatrix} 0 & 1 \\ 1 & -2\gamma\mu_j \end{smallmatrix}\right)$ has determinant -1. Thus no nonzero adjoint eigenmode is invisible on any positive interval. With full-domain distributed control, completeness of the eigenmodes yields the dense-range property for each $\beta > 0$. This modal argument does not extend automatically to localized actuators.

Lemma 3.6 (Regularized terminal steering)**.** *Assume the linear beam system is approximately controllable on $[L-\delta, L]$. Let $y_0 \in \mathbb{U}$ be the state at time $L-\delta$, and let $\widetilde{\omega} \in \mathbb{U}$ be a target. For $r_1 > 0$, define*

$$u_{r_1}^{\delta}(\vartheta) = \mathbb{B}^* S^*(L-\vartheta)(r_1 I + Q_{L\delta})^{-1}(\widetilde{\omega} - S(\delta)y_0). \tag{3.8}$$

Then the corresponding terminal linear state satisfies

$$y_{r_1}^{\delta}(L) - \widetilde{\omega} = -r_1(r_1 I + Q_{L\delta})^{-1}(\widetilde{\omega} - S(\delta)y_0), \tag{3.9}$$

and hence

$$\lim_{r_1 \downarrow 0} \|y_{r_1}^{\delta}(L) - \widetilde{\omega}\|_{\mathbb{U}} = 0. \tag{3.10}$$

Proof. Substitute (3.8) into the mild formula on $[L-\delta, L]$:

$$\begin{aligned} y_{r_1}^{\delta}(L) &= S(\delta)y_0 + G_{L\delta}G_{L\delta}^*(r_1 I + Q_{L\delta})^{-1}(\widetilde{\omega} - S(\delta)y_0) \\ &= S(\delta)y_0 + Q_{L\delta}(r_1 I + Q_{L\delta})^{-1}(\widetilde{\omega} - S(\delta)y_0). \end{aligned}$$

Use the resolvent identity

$$Q_{L\delta}(r_1 I + Q_{L\delta})^{-1} = I - r_1(r_1 I + Q_{L\delta})^{-1}$$

to obtain (3.9). The limit (3.10) is exactly item (v) of Lemma 3.4. □

Remark 3.7 (Control-energy interpretation)**.** *The norm of $u_{r_1}^{\delta}$ does not have to stay uniformly bounded as $r_1 \downarrow 0$. It is not a deficiency; in case of a dense non-closed image of the control map, an approximation of a non-reachable target might require more effort from control due to its density. The importance of the above comment arises because in case the semilinear term explicitly involves the control, the presence of $\|u_{r_1}^{\delta}\|$ multiplied by some constant becomes inevitable.*

4. Approximate controllability of the semilinear beam system

We now return to the full beam problem with delay, memory, and non-instantaneous impulses. The proof separates the already generated trajectory from the last control interval. This section makes that separation explicit and states the technical condition needed when the nonlinearity depends directly on the terminal steering control.

Definition 4.1 (Approximate controllability of the nonlinear system)**.** *System* (2.13) *is approximately controllable on* $[0, L]$ *if, for every initial history* $\Phi \in C([-a, 0]; \mathbb{U})$*, every target* $\widetilde{\omega} \in \mathbb{U}$*, and every* $\varepsilon > 0$*, there exists* $u \in L^2(0, L; \mathbb{X})$ *such that the corresponding mild solution satisfies*

$$\|\omega(L) - \widetilde{\omega}\|_{\mathbb{U}} < \varepsilon.$$

When $L < \ell_1$, no impulse is active before the terminal time, and Definition 4.1 reduces to the usual semilinear beam controllability setting considered in [9]. The interest here is that the same steering idea survives after a finite number of non-instantaneous impulse intervals.

4.1. Why the final control window is shorter than the delay

Lemma 4.2 (History freezing on the terminal window)**.** *Let* $0 < \beta < a$ *and let two controls* u_1, u_2 *coincide on* $[0, L - \beta]$*. Assume that the corresponding mild solutions* $\omega^{(1)}$ *and* $\omega^{(2)}$ *are unique. Then, for every* $\ell \in [L - \beta, L]$*,*

$$\omega^{(1)}(\ell - a) = \omega^{(2)}(\ell - a). \tag{4.1}$$

More generally, every delayed value whose time argument lies at most $\ell - a$ *is determined before the terminal control window begins.*

Proof. If $\ell \in [L - \beta, L]$, then

$$\ell - a \le L - a < L - \beta$$

because $\beta < a$. Thus the value at time $\ell - a$ belongs to the interval on which the controls are identical. Uniqueness of the mild solution up to time $L - \beta$ gives (4.1). □

Remark 4.3. *Lemma 4.2 is the reason for the restriction* $\beta < a$*. If the terminal control window were longer than the delay, then the delayed state* $\omega(\ell - a)$ *could itself depend on the modified terminal control, and the simple small-window estimate used below would no longer isolate the nonlinear contribution. A different fixed-point or feedback argument would then be required.*

4.2. Terminal-window estimates

We first describe the local bounds used in the proof. Because the delayed history is frozen on the last window, its image is contained in a fixed bounded set determined by the trajectory at times not exceeding $L - \beta$.

Assumption 4.4 (Terminal nonlinear and memory bounds)**.** *For every bounded set* K *of delayed values attained before the terminal window, there are constants* $M_F(K) \ge 0$*,* $M_H(K) \ge 0$*, and* $\kappa \ge 0$ *such that on the last evolution interval*

$$\|\mathbb{F}(\ell, \eta, u)\|_{\mathbb{U}} \le M_F(K) + \kappa \|u\|_{\mathbb{X}}, \qquad \eta(-a) \in K, \tag{4.2}$$

and

$$\left\| \int_{\vartheta_N}^{\ell} \mathbb{H}(\ell, m, \eta_m)\, dm \right\|_{\mathbb{U}} \le M_H(K). \tag{4.3}$$

If $\kappa = 0$*, the nonlinear term is uniformly bounded with respect to the control on the terminal window.*

Condition (4.3) follows, for example, from $g \in L^1$ and local boundedness of h along the frozen history. The direct control dependence in (4.2) needs additional care because, as noted in Remark 3.7, the norm of a regularized approximate control may increase as $r_1 \downarrow 0$.

A necessary correction to the original compatibility proposal. For bounded $\mathbb{B}$ and $0 < \beta \le L$, the control map satisfies

$$\|G_{L\beta}u\|_{\mathbb{U}} \le N\|\mathbb{B}\|\sqrt{\beta}\,\|u\|_{L^2(L-\beta,L;\mathbb{X})}. \tag{4.4}$$

Thus imposing $\sqrt{\beta_n}\|u_n\|_{L^2} \to 0$ makes the controlled terminal increment tend to zero; it is *incompatible* with steering a fixed reference state to an arbitrary different target. We therefore withdraw that condition and do not claim a general theorem for a control-dependent perturbation with arbitrary $\kappa > 0$. The result below assumes that the remaining delayed nonlinearity is uniformly bounded in the terminal control ($\kappa = 0$), possibly after absorbing a bounded affine contribution Du into $\mathbb{B}_{\text{eff}} = \mathbb{B} + D$.

Definition 4.5 (Diagonal regularization choice)**.** *Fix a single reference control before the last window and the associated trajectory ω^{ref}. Choose $\beta_n \downarrow 0$ with $0 < \beta_n < \min\{a, L - \vartheta_N\}$. For each n, choose $r_{1,n} > 0$ sufficiently small so that the* fixed-window *Gramian control, initialized at $\omega^{\text{ref}}(L-\beta_n)$, satisfies*

$$\left\| r_{1,n}(r_{1,n}I + Q_{L\beta_n})^{-1}[\widetilde{\omega} - S(\beta_n)\omega^{\text{ref}}(L-\beta_n)] \right\|_{\mathbb{U}} < 1/n. \tag{4.5}$$

Such a choice exists for each fixed $\beta_n > 0$ when the linear pair is approximately controllable on that interval. No small-control-energy assertion is made.

Proposition 4.6 (Vanishing terminal nonlinear remainder)**.** *Assume Assumptions 2.1 and 4.4, with $\kappa = 0$ in* (4.2)*, and let $(\beta_n, r_{1,n})$ be a diagonal choice as in Definition 4.5. Let ω^n be the solution obtained by replacing the original control on $[L-\beta_n, L]$ with $u^{\beta_n}_{r_{1,n}}$, while keeping the original control before $L - \beta_n$. Then the nonlinear and memory contribution accumulated on the terminal interval satisfies*

$$\|\mathbb{R}_n\|_{\mathbb{U}} \longrightarrow 0, \tag{4.6}$$

where

$$\begin{aligned}\mathbb{R}_n = &\int_{L-\beta_n}^{L} S(L-\vartheta)\mathbb{F}(\vartheta, \omega^n_\vartheta, u^{\beta_n}_{r_{1,n}}(\vartheta))\,d\vartheta \\ &+ \int_{L-\beta_n}^{L} S(L-\vartheta)\int_{\vartheta_N}^{\vartheta} \mathbb{H}(\vartheta, m, \omega^n_m)\,dm\,d\vartheta.\end{aligned} \tag{4.7}$$

Proof. By Lemma 4.2, all delayed states entering $\mathbb{F}$ and $\mathbb{H}$ on $[L-\beta_n, L]$ have delayed values in a fixed bounded set K generated by the one reference trajectory before terminal steering. Using (2.7) and (4.2),

$$\left\| \int_{L-\beta_n}^{L} S(L-\vartheta)\mathbb{F}(\vartheta, \omega^n_\vartheta, u^{\beta_n}_{r_{1,n}}(\vartheta))\,d\vartheta \right\| \le NM_F(K)\beta_n. \tag{4.8}$$

This is $O(\beta_n)$, because the delayed values are taken from the same uniformly bounded reference trajectory. The corresponding estimate with $\kappa > 0$ cannot be made small by a vanishing-energy hypothesis without destroying the linear terminal steering effect. Similarly, (4.3) gives

$$\left\| \int_{L-\beta_n}^{L} S(L-\vartheta)\int_{\vartheta_N}^{\vartheta} \mathbb{H}(\vartheta, m, \omega^n_m)\,dm\,d\vartheta \right\| \le NM_H(K)\beta_n \longrightarrow 0. \tag{4.9}$$

Combining (4.8) and (4.9) proves (4.6). □

4.3. Main controllability theorem

Theorem 4.7 (Approximate controllability of the semilinear impulsive beam)**.** *Assume Assumptions 2.1 and 4.4. Suppose* $\kappa = 0$ *in* (4.2) *or that an affine control perturbation has been absorbed into a bounded effective control operator. Assume that the resulting effective linear pair is approximately controllable on every sufficiently short terminal interval* $[L-\beta, L]$*. Then the full semilinear system is approximately controllable on* $[0, L]$*.*

Proof. Let $\varepsilon > 0$, fix an initial history Φ, and let $\widetilde{\omega} \in \mathbb{U}$ be arbitrary. We organize the argument in five steps.

Step 1: generate the reference trajectory before the terminal window. Choose the diagonal family $(\beta_n, r_{1,n})$ of Definition 4.5 with $\beta_n < \min\{a, L-\vartheta_N\}$. Fix a single reference control u^{ref} on $[0, L]$ and let ω^{ref} denote its unique trajectory. On every initial segment $[0, L-\beta_n]$, use the restriction of this same control, so the delayed values lie on one fixed bounded trajectory. The condition $L-\beta_n > \vartheta_N$ ensures that the terminal steering takes place after the last non-instantaneous impulse.

Step 2: replace the control only on the final interval. Define

$$\widehat{u}_n(\ell) = \begin{cases} u^{\mathrm{ref}}(\ell), & 0 \le \ell \le L-\beta_n, \\ u^{\beta_n}_{r_{1,n}}(\ell), & L-\beta_n < \ell \le L, \end{cases} \tag{4.10}$$

where $u^{\beta_n}_{r_{1,n}}$ is the regularized control of Lemma 3.6 with initial state $\omega^{\mathrm{ref}}(L-\beta_n)$. Let ω^n denote the mild solution corresponding to $\widehat{u}_n$.

Step 3: identify the linear steering part. By the semigroup property, the terminal value can be decomposed as

$$\omega^n(L) = y^{\beta_n}_{r_{1,n}}(L) + \mathbb{R}_n, \tag{4.11}$$

where $y^{\beta_n}_{r_{1,n}}(L)$ is the terminal state of the linear system starting from $\omega^{\mathrm{ref}}(L-\beta_n)$ and $\mathbb{R}_n$ is exactly the nonlinear remainder defined in (4.7). The previous impulse intervals are already contained in the state $\omega^{\mathrm{ref}}(L-\beta_n)$; no impulse term is generated inside the final window.

Step 4: make both errors small. The diagonal choice in (4.5) gives

$$\|y^{\beta_n}_{r_{1,n}}(L) - \widetilde{\omega}\|_{\mathbb{U}} \longrightarrow 0.$$

Proposition 4.6 gives

$$\|\mathbb{R}_n\|_{\mathbb{U}} \longrightarrow 0.$$

Hence, for all sufficiently large n, each quantity is smaller than $\varepsilon/2$.

Step 5: conclude by the triangle inequality. Using (4.11),

$$\|\omega^n(L) - \widetilde{\omega}\|_{\mathbb{U}} \le \|y^{\beta_n}_{r_{1,n}}(L) - \widetilde{\omega}\|_{\mathbb{U}} + \|\mathbb{R}_n\|_{\mathbb{U}} < \varepsilon.$$

Since the target and tolerance were arbitrary, Definition 4.1 is satisfied. □

Corollary 4.8 (Affine control perturbations)**.** *Suppose* $\mathbb{F}(\ell, \eta, u) = \mathbb{F}_0(\ell, \eta) + Du$ *with a bounded operator* $D : \mathbb{X} \to \mathbb{U}$ *and with* $\mathbb{F}_0$ *uniformly bounded on bounded delayed-state sets. If* $(\mathbb{A}, \mathbb{B} + D)$ *is approximately controllable on all sufficiently short terminal intervals, Theorem 4.7 applies after replacing* $\mathbb{B}$ *by* $\mathbb{B} + D$*. In particular, the illustrative term* $0.05u$ *in the velocity forcing is absorbed into* $1.05\mathbb{B}$*. This is a sufficient structural condition, not a result for arbitrary nonlinear dependence on the control.*

Remark 4.9 (Limitations for nonlinear control dependence)**.** *For a general perturbation satisfying only* $\|\mathbb{F}\| \le M_F + \kappa\|u\|$, $\kappa > 0$*, the present terminal-window proof does not establish controllability. The original small-energy schedule would also force the linear steering contribution to vanish by* (4.4)*. A separate robust controllability or fixed-point argument is required to extend the theorem to such perturbations.*

Remark 4.10 (Role of compactness)**.** *Compactness of the beam semigroup is not used to claim exact controllability. On the contrary, it explains why approximate controllability is the appropriate notion. The key analytical property is the strong resolvent limit in Lemma 3.4, which expresses density of the reachable set despite the compactness of the control operator.*

5. Numerical methodology and computational illustration

5.1. Purpose, model, and reproducibility boundary

The following newly computed experiments implement a *time-discrete regularized controllability Gramian for every spatial sine mode* of the full-domain-controlled finite-difference beam. This supersedes the original hard-coded terminal-error and timing arrays and the subsequent lagged-feedback experiments. Unlike the earlier two-mode diagnostic, the test retains all $M - 1$ spatial degrees of freedom, a nonlinear delayed forcing, a fading-memory variable, and a finite-duration impulse *before* the terminal control window. The program then forward-propagates the controlled full-grid equation and checks its terminal state independently of the Gramian residual formula. These observations concern the specified finite-dimensional benchmark and do not independently establish the infinite-dimensional theorem.

Let $\Omega = (0, \pi)$ with hinged endpoints $q = \Delta q = 0$. The benchmark parameters are summarized in Table 1. During ordinary evolution the benchmark is

$$q_{\ell\ell} + 2\gamma(-\Delta)q_\ell + (-\Delta)^2 q = 1.05u + 0.1\sin(q(\ell - a, \varpi)) + H(\ell, \varpi), \tag{5.1}$$

where

$$H(\ell, \varpi) = \int_{\sigma(\ell)}^{\ell} e^{-d(\ell - s)} \frac{q(s - a, \varpi)^3}{1 + q(s - a, \varpi)^2}\, ds. \tag{5.2}$$

Here $\sigma(\ell) = 0$ before the impulse, and $\sigma(\ell) = \vartheta_1$ after the impulse: *memory is restarted after the interval impulse*. The affine $0.05u$ perturbation has been absorbed into the control gain 1.05, as permitted by the conditional analytical result. On $(\ell_1, \vartheta_1]$, the differential equation is suspended, and the explicit non-instantaneous impulse profile is $q_\ell = 0.2\sin q$, with zero impulse input and a continuous displacement update. The one-sided velocity may jump at switching boundaries. The numerical history is held constant, $q(\ell, \varpi) = 0.2\sin\varpi$ for $-a \le \ell \le 0$, with $q_\ell(0, \varpi) = 0$. The terminal target is $(\widetilde{q}, \widetilde{v}) = (0.5\sin(2\varpi), 0)$. The initial and target velocities are both zero. The constant negative-time history, nonlinear impulse-velocity law, and memory restart are explicitly specified assumptions of this numerical benchmark; they have not been calibrated to a physical structure.

Table 1. Explicit benchmark parameters for the full-grid regularized Gramian.

Parameter	Value	Parameter	Value
Domain Ω	$(0,\pi)$	Final time L	1
Damping γ	1.5	Delay a	0.2
Impulse starts ℓ_1	0.3	Impulse ends ϑ_1	0.5
Control window β	0.1	Memory decay d	1
Impulse coefficient	0.2	Effective distributed gain	1.05
Baseline spatial intervals M	100	Baseline time steps N_ℓ	2000

Computational implementation and reproducibility. The calculations were performed in MATLAB R2025b using double-precision arithmetic. Each regularized two-by-two modal system is solved directly without an iterative stopping tolerance. The numerical algorithm, benchmark parameters, time-integration formula, delay and memory conventions, and residual definitions are stated in this section. A self-contained MATLAB R2025b source file, `SUPPLEMENTARY_MATH30865.m`, is provided separately as a computational supplementary file; running it regenerates the numerical data tables and five figures from the specified benchmark equations. The submitted file contains executable source code rather than pre-entered numerical result arrays. No processor-dependent timing benchmark or unrecorded hardware specification is claimed.

The terminal control interval $[0.9, 1]$ lies after the impulse and has length $\beta = 0.1 < a = 0.2$. Thus delayed values on the terminal interval are sampled strictly before time 0.9 and are fixed by the already simulated uncontrolled trajectory. The delayed memory integrand is frozen in the same way, although its integral keeps evolving. These restrictions make the terminal discrete system affine in the distributed control.

5.2. Spatial energy norm and stable time discretization

For M equal spatial subintervals, set $h = \pi/M$ and let A_h be the standard positive Dirichlet second-difference matrix. Write $K_h = A_h^2$, $C_h = 2\gamma A_h$ and use implicit midpoint for the ordinary evolution, with the delayed nonlinear forcing evaluated from the stored history. If (q_n, v_n) denotes the grid displacement and velocity and $f_{n+1/2}$ the known midpoint forcing, the update is

$$\begin{aligned}(I + \tfrac{\Delta\ell}{2}C_h + \tfrac{\Delta\ell^2}{4}K_h)v_{n+1} &= (I - \tfrac{\Delta\ell}{2}C_h - \tfrac{\Delta\ell^2}{4}K_h)v_n - \Delta\ell K_h q_n + \Delta\ell f_{n+1/2},\\ q_{n+1} &= q_n + \tfrac{\Delta\ell}{2}(v_n + v_{n+1}).\end{aligned} \tag{5.3}$$

The coefficient matrix is positive definite, and its Cholesky factors are reused. Exponential memory is advanced by exact exponential weights under piecewise-constant delayed integrands. On the impulse interval, $q_{n+1} = q_n + \Delta\ell\, 0.2\sin(q_n)$ with the corresponding prescribed velocity; the memory state is reset. The impulse update is first-order even though the linear ordinary-stage method is implicit midpoint.

In particular, the old explicit-biharmonic stability restriction $\Delta\ell\lambda_{\max}(A_h) \le 2$ is violated on three of the four previously published coupled grids (approximately 2.026, 4.053, and 8.106). Accordingly, the old error and runtime tables are not used as numerical evidence in this revision. The new calculations use the method (5.3), not the former explicit recurrence.

The natural discrete norms at terminal time are

$$E_q = (h\sum_i |q_i - \widetilde{q}_i|^2)^{1/2}, \quad E_v = (h\sum_i |v_i - \widetilde{v}_i|^2)^{1/2}, \quad E_{\mathbb{U}} = (h\|A_h(q-\widetilde{q})\|_2^2 + E_v^2)^{1/2}. \tag{5.4}$$

The two velocity conditions are zero, but E_v is still calculated and reported; displacement error alone is not the product-space error.

5.3. Finite-grid regularized Gramian control

Let λ_k be an eigenvalue of A_h and write the energy-scaled modal state $z_k = (\lambda_k \widehat{q_k}, \widehat{v_k})^T$. The terminal linear evolution on each spatial mode is

$$\dot{z}_k = \mathcal{A}_k z_k + \mathcal{B}_k \widehat{u}_k + \widehat{f_k}, \qquad \mathcal{A}_k = \begin{pmatrix} 0 & \lambda_k \\ -\lambda_k & -2\gamma\lambda_k \end{pmatrix}, \quad \mathcal{B}_k = \begin{pmatrix} 0 \\ 1.05 \end{pmatrix}. \tag{5.5}$$

Writing $d = \Delta\ell$ for the time increment within this paragraph, the implicit-midpoint step yields

$$F_k = (I - d\mathcal{A}_k/2)^{-1}(I + d\mathcal{A}_k/2), \qquad B_k = (I - d\mathcal{A}_k/2)^{-1} d\mathcal{B}_k.$$

For the n_w terminal input stages, define $G_k = [F_k^{n_w-1} B_k, \ldots, B_k]$ and the discrete Gramian $Q_k = G_k G_k^T/d$. If d_k is the difference between the desired terminal mode and the uncontrolled terminal mode with its *known* history forcing, the controls are

$$U_{k,\eta} = G_k^T (Q_k + \eta I)^{-1} d_k/d, \qquad \eta > 0. \tag{5.6}$$

The exact finite-grid predicted modal residual is $-\eta(Q_k + \eta I)^{-1} d_k$. Every one of the $M - 1$ modes is retained, so the computation is a full *spatial-grid* Gramian, rather than a two-mode reduction. The resulting modal controls are transformed back to physical grid controls; the nonlinear delayed beam, impulse history and fading memory are retained in the forward propagation.

5.4. Regularization results and control cost

MATLAB R2025b (double precision) generated the full-mode tables and figures on 9 October 2026. The main experiment uses $(M, N_\ell) = (100, 2000)$, $n_w = 200$ terminal control stages, and $\eta \in \{10^{-2}, 10^{-3}, \ldots, 10^{-8}\}$. Table 2 is transcribed from the comma-separated values (CSV) file produced by the supplied implementation, without pre-entered error values.

Table 2. Full-grid Gramian: terminal displacement, velocity and energy errors, and L^2 control cost.

η	E_q	E_v	$E_{\mathbb{U}}$	$\|u\|_{L^2}$
10^{-2}	0.596111	0.306055	2.205007	7.978500
10^{-3}	0.352742	0.184681	1.114048	38.843070
10^{-4}	0.137948	0.031948	0.223332	65.553682
10^{-5}	0.025147	0.003574	0.031417	72.829631
10^{-6}	0.002753	0.000364	0.003343	74.068415
10^{-7}	0.000278	0.00003648	0.000337	74.204470
10^{-8}	0.00002782	0.000003648	0.00003368	74.218214

The product-space error decreases from 2.205007 to 3.3683×10^{-5} between $\eta = 10^{-2}$ and $\eta = 10^{-8}$, as shown in Figure 1; Figure 2 shows the corresponding rise in the L^2 control norm from

7.9785 to about 74.2182. The numerical control cost should not be assumed uniformly bounded for arbitrary infinite-dimensional targets or finer spatial discretizations. Within each run, the Gramian-predicted errors agree with the terminal errors obtained by forward propagation; the largest reported relative product-energy mismatch in the baseline full run is 3.64×10^{-13}. This checks the algebraic consistency of the controller and the discrete beam integrator using the same numerical model; it is not an independent convergence proof for the PDE.

Figure 3 compares the terminal displacement with the prescribed target and uncontrolled profile.

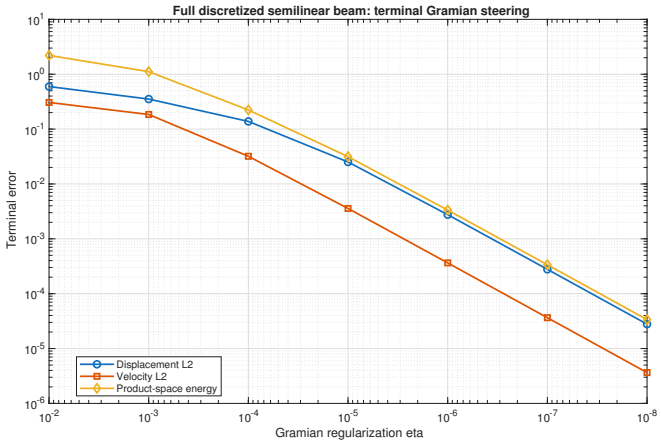


Figure 1. Finite-grid terminal errors under decreasing Gramian regularization. The complete product-space norm is plotted alongside displacement and velocity errors.

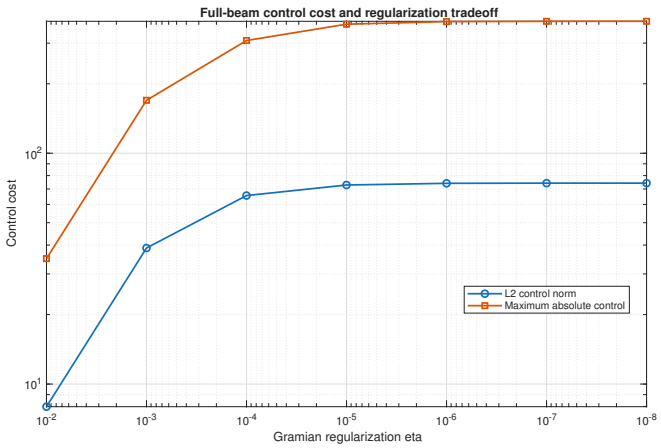


Figure 2. Control cost and peak control magnitude versus Gramian regularization. Smaller errors require larger controls in this benchmark.

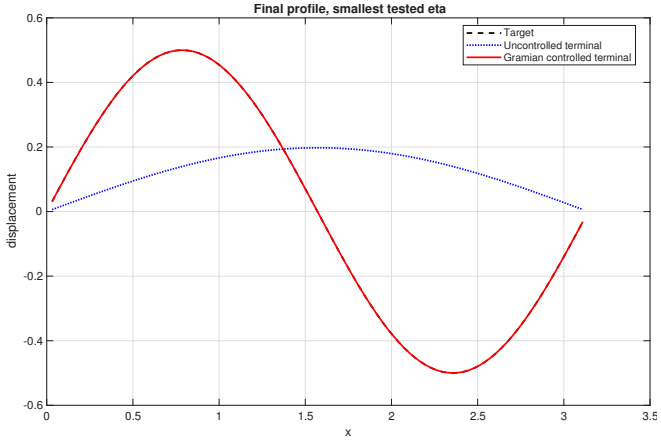


Figure 3. Terminal displacement at the smallest reported regularizer, compared with the prescribed target and the uncontrolled terminal profile.

5.5. Grid refinement and parameter sensitivity

To separate resolution effects from regularization effects, we hold $\eta = 10^{-6}$ fixed and recompute on four coupled spatial/time grids, as reported in Table 3. Their nonzero errors remain nearly constant because the regularization is fixed; this is *grid consistency*, not an estimate of the order of truncation error or a proof that the target residual tends to zero with mesh refinement.

Table 3. Coupled spatial/time refinement for the full-grid Gramian at $\eta = 10^{-6}$.

M	N_ℓ	E_q	E_v	$E_{\mathbb{U}}$
25	500	0.002761668	0.000364200	0.003351799
50	1000	0.002754595	0.000364069	0.003345040
100	2000	0.002752839	0.000364037	0.003343362
200	4000	0.002752405	0.000364029	0.003342947

Figure 4 visualizes the terminal errors across these coupled grids.

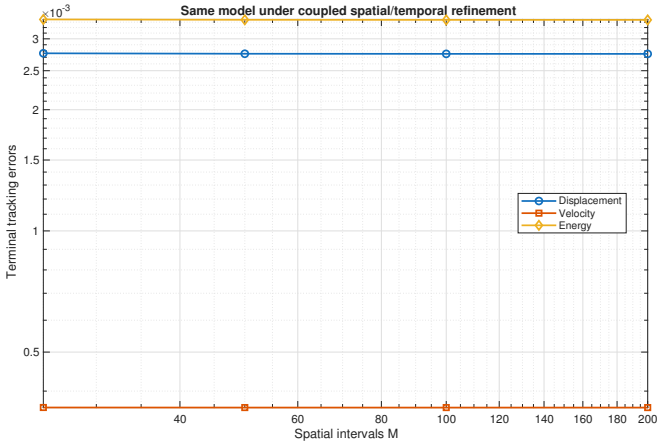


Figure 4. Terminal tracking errors under coupled spatial/time refinement with a fixed regularizer.

Parameter sensitivity is assessed by changing one value at a time, recomputing the Gramian and reporting the new controlled residual rather than reusing the baseline controller. For all rows in Table 4 the spatial/time grid is $(50, 1000)$ and $\eta = 10^{-6}$.

Table 4. One-at-a-time parameter sensitivity in the full spatial Gramian calculation.

Scenario	$E_{\mathbb{U}}$	$\|\|u\|\|_{L^2}$
Baseline	0.00334504	74.06323
Damping $\gamma = 1.8$	0.00342186	75.96720
Delay $a = 0.16$	0.00334514	74.06363
Memory decay $d = 0.5$	0.00334508	74.06340
Impulse end $\vartheta_1 = 0.55$	0.00338544	74.22992
Impulse coefficient 0.3	0.00344423	74.47540
Effective control gain 1.0	0.00368510	77.75027

Figure 5 presents the corresponding changes in the three terminal errors.

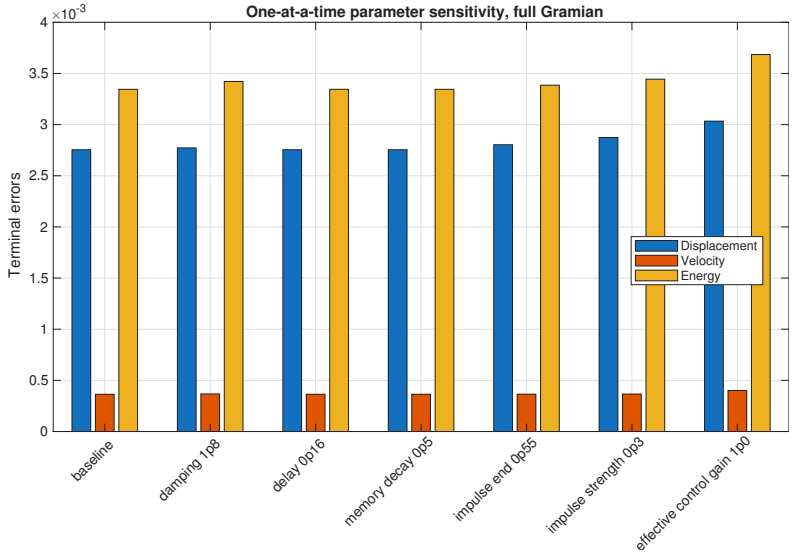


Figure 5. Sensitivity of the terminal displacement, velocity, and energy errors in the full-grid Gramian test.

5.6. Numerical scope and outstanding model verification

The sampled modes and finite-grid Gramian are controllable in this fully distributed-actuator setup; the smallest eigenvalue of its regularized terminal Gramian before adding ηI was approximately 4.535×10^{-5} on the baseline grid. The maximum relative sine-transform orthogonality defect was below 10^{-14}. These checks make the computation internally reproducible and demonstrate terminal numerical tracking for the *specified* control-affine benchmark with frozen terminal history. They do not establish that arbitrary nonlinear, control-dependent perturbations are admissible, that a spatially localized actuator gives the same result, or that the infinite-dimensional theorem follows from any fixed grid. The impulse-velocity law, initial history, and memory-reset rule are treated as explicitly defined benchmark assumptions; no fit to a physical device or empirical data is asserted.

The computations use full-domain distributed control and a final control interval following all impulse intervals.

6. Discussion of the analytical assumptions and scope

The preceding analysis uses several assumptions that have distinct purposes. Since these assumptions can easily be confused when the beam, delay, memory, and impulse mechanisms are written in one equation, this section explains their role and the consequences of relaxing them.

6.1. Why approximate controllability is used instead of exact controllability

In the case of the linearized beam, the terminal control map $G_{L\delta}$ involves the compact semigroup $S(L-\vartheta)$ for positive time. For an infinite-dimensional Hilbert space, this would be a serious obstacle to the exact surjectivity of the control operator. Approximate controllability bypasses the obstacle through the requirement

$$\overline{\text{Range}(G_{L\delta})} = \mathbb{U}.$$

It follows that the regularized inverse $(r_1 I + Q_{L\delta})^{-1}$ is not an approximation of the everywhere defined inverse of $Q_{L\delta}$, but is a tool that chooses controls having their end defects vanishing as $r_1 \downarrow 0$ strongly. It is this which causes the control norm to be large when the target is outside the range but within its closure.

6.2. Role of the delay inequality $\beta < a$

The inequality $\beta < a$ is structural, not cosmetic. It ensures that the delayed state in the last window is already known. If $\beta = a$, the endpoint $\ell = L$ accesses the state at $L - a = L - \beta$, which is exactly the switching time; the argument can still be treated with one-sided continuity, but the strict inequality avoids endpoint ambiguity. If $\beta > a$, then for times near L, the delayed argument $\ell - a$ lies inside the terminal control window and is altered by the new steering control. The frozen-history estimate of Lemma 4.2 then fails.

This does not imply that controllability cannot be achieved in case $\beta \geq a$; it only implies that the current proof technique is insufficient. To do that, one will have to estimate the difference between the two terminal trajectories via a contraction/compactness/Gronwall argument which takes into account the feedback of the terminal control via the delay.

6.3. Memory does not behave like a single discrete delay

The memory contribution integrates the complete past over an interval. Consequently, even when the delayed point $\ell - a$ is frozen, the memory term does not vanish. The proof instead uses the fact that the outer integration interval has length β. If the inner memory integral is uniformly bounded, the total terminal memory residual is $O(\beta)$. This is precisely the content of (4.9).

The assumption $g \in L^1(0, L)$ is natural for fading-memory kernels. Exponential kernels, sums of exponentials, and many viscoelastic relaxation kernels satisfy it. Kernels with a non-integrable singularity would require a different functional setting, for example fractional resolvent families or weighted history spaces.

6.4. Non-instantaneous impulses and the location of the terminal window

Choosing $\beta < L - \vartheta_N$ ensures that the control interval comes strictly after the last impulse interval. Hence, the state at $L - \beta$ would include the effect of all impulses, but there will be no impulse during the application of the Gramian control. If an impulse coincides with the control interval, then the evolution would follow Ψ_N in part of the interval, so the linear control map $G_{L\beta}$ no longer gives the complete terminal evolution map. The proof of controllability under these conditions would require an impulse-dependent terminal map.

6.5. Direct dependence of the nonlinearity on the control

The bounded-control map estimate (4.4) shows that a requirement of the form $\sqrt{\beta}\|u\|_{L^2} \to 0$ cannot coexist with arbitrary terminal steering from a fixed reference state. We explicitly retract the unrestricted $\kappa > 0$ claim and prove the result for control-independent/uniformly bounded delayed perturbations. An affine term Du can be included in $\mathbb{B}_{\text{eff}} = \mathbb{B} + D$ if dense range of the resulting effective pair is verified; nonlinear control dependence is left open.

6.6. Relationship to tempered fractional impulsive controllability

The tempered fractional model of Guo, Zhang, and Li [19] accounts for attenuation directly in a fractional kernel, whereas the present beam includes a fading hereditary convolution alongside an integer-order, second-order structural evolution. The associated solution operators, Gramian, and regularity estimates cannot be interchanged without additional analysis. Similarly, the non-instantaneous fractional systems in [21, 22] support the relevance of impulsive delayed dynamics but do not verify our beam-specific control assumptions. These distinctions limit the reach of the current theorem and clarify the relation to recent research.

6.7. Interpretation of the numerical evidence

The newly executed spatial-grid Gramian experiment is now directly tied to the controller of the analytical argument in the special control-affine, terminal-history-frozen benchmark. It yields decreasing terminal displacement, velocity and product-energy errors as $\eta \to 0$ on each fixed finite grid, at an increasing control cost. It replaces both the original hard-coded plot arrays and the earlier full-beam feedback experiment whose residual plateaued. The fully distributed finite-dimensional Gramian, however, is a more favorable setting than an arbitrary infinite-dimensional actuator, so these figures are reproducible computational illustrations rather than proofs of the abstract theorem.

7. Conclusions

The present study investigates conditional approximate controllability of a damped Euler–Bernoulli beam with memory, delayed nonlinearities, and non-instantaneous impulses. The short terminal window is chosen after all impulse intervals and shorter than the delay, so that its delayed contributions can be bounded independently of the last-window control. The analytical conclusion requires dense linear reachability and appropriate control-independent or effectively affine nonlinear bounds; the previously proposed vanishing-control-energy compatibility claim is not retained.

New MATLAB R2025b tests implement a Tikhonov-regularized Gramian for every spatial mode of a fully distributed beam discretization. On the baseline grid, the displacement, velocity and product-energy terminal errors decrease together as the regularizer is reduced, and the predicted residual agrees with direct full-grid propagation. The experiments quantify the associated control cost and show stable results under coupled mesh refinement and moderate parameter perturbations. This resolves the previous discrepancy between the analytical Gramian controller and the numerical feedback law for this specified finite-dimensional benchmark. It does not turn numerical convergence into a proof of the infinite-dimensional theorem. The impulse-velocity profile, constant negative-time history, and memory-reset rule are prescribed benchmark conventions, not experimentally verified physical laws; extensions to other impulse conventions, persistent memory, and restricted actuator regions remain open.

Author contributions

All authors contributed to the development of the study, analysis of the results, and preparation and revision of the manuscript.

Use of Generative-AI tools declaration

The authors declare that they have not used Artificial Intelligence (AI) tools in the creation of this article.

Funding

Ongoing Research Funding program, (ORF-2026-1557), King Saud University, Riyadh, Saudi Arabia.

Conflict of interest

The authors declare they have no conflicts of interest in this paper.

References

1. L. H. Eliasson, B. Grébert, S. B. Kuksin, KAM for the nonlinear beam equation, *Geom. Funct. Anal.*, **26** (2016), 1588–1715. https://doi.org/10.1007/s00039-016-0390-7
2. A. S. Ackleh, H. T. Banks, G. A. Pinter, A nonlinear beam equation, *Appl. Math. Lett.*, **15** (2002), 381–387. https://doi.org/10.1016/S0893-9659(01)00147-1
3. J. N. Franklin, R. F. Scott, Beam equation with variable foundation coefficient, *J. Eng. Mech. Div.*, **105** (1979), 811–827. https://doi.org/10.1061/JMCEA3.0002525
4. E. Hernández, D. O'Regan, On a new class of abstract impulsive differential equations, *Proc. Amer. Math. Soc.*, **141** (2013), 1641–1649. https://doi.org/10.1090/S0002-9939-2012-11613-2

5. S. Lalvay, A. Padilla-Segarra, W. Zouhair, On the existence and uniqueness of solutions for non-autonomous semilinear systems with non-instantaneous impulses, delay, and nonlocal conditions, *Miskolc Math. Notes*, **23** (2022), 295–310. http://doi.org/10.18514/MMN.2022.3785
6. Y. Chen, K. Meng, Stability and solvability for a class of optimal control problems described by non-instantaneous impulsive differential equations, *Adv. Differ. Equ.*, **2020** (2020), 524. https://doi.org/10.1186/s13662-020-02919-z
7. E. Zuazua, Exact controllability for the semilinear wave equation, *J. Math. Pures Appl.*, **69** (1990), 1–31.
8. J. Lagnese, J. L. Lions, *Modelling, analysis and control of thin plates*, Paris: Masson, 1988.
9. A. Carrasco, H. Leiva, J. Sanchez, Controllability of the semilinear beam equation, *J. Dyn. Control Syst.*, **19** (2013), 553–568. https://doi.org/10.1007/s10883-013-9193-4
10. J. A. Asadzade, N. I. Mahmudov, Approximate controllability of impulsive semilinear evolution equations in Hilbert spaces, *Int. J. Control*, **99** (2026), 336–357. https://doi.org/10.1080/00207179.2025.2516182
11. S. Priyadharshini, S. S. Santra, V. Sadhasivam, D. Majumder, P. Dhali, Forced oscillation of certain class of impulsive Euler–Bernoulli beam equations with damping term, In: *Advances in mathematical modelling, applied analysis and computation*, Springer, Cham, 2025, 150–159. https://doi.org/10.1007/978-3-031-90917-7_10
12. A. E. Bashirov, N. Ghahramanlou, On partial approximate controllability of semilinear systems, *Cogent Eng.*, **1** (2014), 965947. https://doi.org/10.1080/23311916.2014.965947
13. A. Kumar, R. K. Vats, A. Kumar, D. N. Chalishajar, Numerical approach to the controllability of fractional order impulsive differential equations, *Demonstr. Math.*, **53** (2020), 193–207. https://doi.org/10.1515/dema-2020-0015
14. A. Anguraj, S. Kanjanadevi, Existence of mild solutions of abstract fractional differential equations with non-instantaneous impulsive conditions, *J. Stat. Sci. Appl.*, **4** (2016), 53–64. https://doi.org/10.17265/2328-224X/2016.0102.004
15. P. Kumar, R. K. Vats, A. Kumar, Result on controllability of Hilfer fractional integro-differential equations of Sobolev type with non-instantaneous impulses, *Filomat*, **37** (2023), 10033–10053. https://doi.org/10.2298/FIL2329033K
16. V. Vijayakumar, R. Udhayakumar, Y. Zhou, N. Sakthivel, Approximate controllability results for Sobolev-type delay differential systems of fractional order without uniqueness, *Numer. Meth. Part. Differ. Equ.*, **39** (2023), 3479–3498. https://doi.org/10.1002/num.22642
17. L. Sadek, A. Toukmati, Controllability of infinite-dimensional conformable Θ-H-systems, *Asian J. Control*, **28** (2026), 124–137. https://doi.org/10.1002/asjc.3659
18. L. Sadek, A. Shafee, I. L. Popa, Exact controllability of linear ψ-fractional control systems, *Results Control Optim.*, **23** (2026), 100703. https://doi.org/10.1016/j.rico.2026.100703
19. L. Guo, B. Zhang, C. Li, The controllability for the tempered fractional-order equation subjected to nonlocal delay and impulsive conditions, *Indian J. Pure Appl. Math.*, 2026. https://doi.org/10.1007/s13226-026-00941-7

20. S. Kumar, Approximate controllability of nonlocal impulsive fractional order semilinear time varying delay systems, *Nonlinear Dyn. Syst. Theor.*, **16** (2016), 420–430.

21. S. Arora, M. T. Mohan, J. Dabas, Approximate controllability of fractional order non-instantaneous impulsive functional evolution equations with state-dependent delay in Banach spaces, *IMA J. Math. Control Inform.*, **39** (2022), 1103–1142. https://doi.org/10.1093/imamci/dnac024

22. A. Kumar, A. Kumar, R. K. Vats, P. Kumar, Approximate controllability of neutral delay integro-differential inclusion of order $\alpha \in (1, 2)$ with non-instantaneous impulses, *Evol. Equ. Control The.*, **11** (2022), 1635–1654. https://doi.org/10.3934/eect.2021058

23. M. Pierri, D. O'Regan, V. Rolnik, Existence of solutions for semilinear abstract differential equations with non-instantaneous impulses, *Appl. Math. Comput.*, **219** (2013), 6743–6749. https://doi.org/10.1016/j.amc.2012.12.084

24. R. F. Curtain, A. J. Pritchard, *Infinite dimensional linear systems theory*, Berlin: Springer, 1978. https://doi.org/10.1007/BFb0006761

25. R. F. Curtain, H. Zwart, *An introduction to infinite-dimensional linear systems theory*, New York: Springer, 1995. https://doi.org/10.1007/978-1-4612-4224-6

26. H. Leiva, N. Merentes, J. Sanchez, A characterization of semilinear dense range operators and applications, *Abstr. Appl. Anal.*, **2013** (2013), 729093. https://doi.org/10.1155/2013/729093



AIMS Press

© 2026 the Author(s), licensee AIMS Press. This is an open access article distributed under the terms of the Creative Commons Attribution License (https://creativecommons.org/licenses/by/4.0)